Geomechanics and Engineering, *Vol. 32, No. 3 (2023) 347-359*
https://doi.org/10.12989/gae.2023.32.3.347

Study on mechanical properties of Yellow River silt solidified by MICP technology

Yuke Wang[1,2,3], Rui Jiang[1,2,3], Gan Wang[1,2,3] and Meiju Jiao*[1]

[1]College of Water conservancy Science and Engineering, Zhengzhou University, Zhengzhou, 450001, China
[2]National Local Joint Engineering Laboratory of Major Infrastructure Testing and Rehabilitation Technology, Zhengzhou 450001, China
[3]Collaborative Innovation Center of Water Conservancy and Transportation Infrastructure Safety Protection, Henan Province, Zhengzhou, 450001, China

(*Received December 6, 2021, Revised January 11, 2023, Accepted January 19, 2023*)

Abstract. With the development of infrastructure, there is a critical shortage of filling materials all over the word. However, a large amount of silt accumulated in the lower reaches of the Yellow River is treated as waste every year, which will cause environmental pollution and waste of resources. Microbial induced calcium carbonate precipitation (MICP) technology, with the advantage of efficient, economical and environmentally friendly protection, is selected to solidify the abandoned Yellow River silt with poor mechanical properties into high-quality filling material in this paper. Based on unconfined compressive strength (UCS) test, determination of calcium carbonate ($CaCO_3$) content and scanning electron microscope (SEM) test, the effects of cementation solution concentration, treatment times and relative density on the solidification effect were studied. The results show that the loose silt particles can be effectively solidified together into filling material with excellent mechanical properties through MICP technology. The concentration of cementation solution have a significant impact on the solidification effect, and the reasonable concentration of cementation solution is 1.5 mol/L. With the increase of treatment times, the pores in the soil are filled with $CaCO_3$, and the UCS of the specimens after 10 times of treatment can reach 2.5 MPa with a relatively high $CaCO_3$ content of 26%. With the improvement of treatment degree, the influence of relative density on the UCS increases gradually. Microscopic analysis revealed that after MICP reinforcement, $CaCO_3$ adhered to the surface of soil particles and cemented with each other to form a dense structure.

Keywords: calcium carbonate content; filling material; MICP; unconfined compressive strength; Yellow River silt

1. Introduction

With the development of society, a large amount of new buildings have an increasing demand for filling material. In order to reduce the exploitation of natural resources, it is necessary to recycle waste to the greatest extent. According to statistics, the average silt discharge of the Yellow River for many years is as much as 1.6 billion tons, especially in the lower reaches, about 400 million tons are deposited every year.

The large amount of accumulated Yellow River silt will not only occupy a lot of land resources, but also cause environmental pollution. However, the Yellow River silt is characterized by small particle size and high silt content, so that it cannot be used as filling material (Wang *et al*. 2022a). In order to use the Yellow River silt as an excellent filling material, the mechanical properties of Yellow River silt must be strengthened. Generally, soil is improved by a series of methods, including preloading consolidation, vibroflotation compaction, grouting, dynamic compaction (Montoya and DeJong 2015). However, these methods generally have the disadvantages of high cost and long construction period, and the treatment effect also has many disadvantages (DeJong *et al.* 2008). Therefore, exploring a new, efficient, economical and environmentally friendly treatment method has become an urgent problem to be solved.

Microbial induced calcite precipitation (MICP) as a new soil improvement technology has been highly concerned by many scholars in recent years (Whiffin 2004, Simatupang *et al.* 2018, Zamani *et al.* 2021, Sharma *et al.* 2022a, b). In most previous studies, Bacillus pasteurium, which can produce highly active urease, has been applied in MICP technology (Mahawish *et al.* 2019). The principle is that urea is hydrolyzed by urease secreted by microorganisms to create an alkaline environment and ammonium ions. Bacteria are employed as the center to induce the production of $CaCO_3$ crystals with the addition of calcium salt. Finally, the loose soils are gradually bonded into a whole with certain strength with the coalescence and adhesion of $CaCO_3$ crystals *et al.* 2019). The chemical reactions involved in the whole process can be summarized as the following formulas.

$$CO(NH_2)_2 + 2H_2O \xrightarrow{\text{urease}} 2NH_4^+ + CO_3^{2-} \tag{1}$$

$$Ca^{2+} + CO_3^{2-} \xrightarrow{\text{nucleation}} CaCO_3 \downarrow \tag{2}$$

MICP technology obviously has the advantages of simple technology, small construction disturbance and ecological environmental protection compared with the traditional methods. Therefore, it is widely used in various

*Corresponding author, Associate Professor
E-mail: Jiaomj@zzu.edu.cn

ISSN: 2005-307X (Print), 2092-6219 (Online)

Table 1 Physical parameters of silt

ω_L (%)	ω_P (%)	G_s	ρ_{dmax} (g·cm^{-3})	ρ_{dmin} (g·cm^{-3})	e_{max}	e_{min}
23.8	12.4	2.7	1.66	1.36	0.99	0.63

related fields, such as foundation reinforcement (Atefeh *et al.* 2021, van Paassen *et al.* 2010), easily liquefied sand treatment (Burbank *et al.* 2011, Montoya *et al.* 2013), anti-seepage of geotechnical structure (Hang *et al.* 2019, Sharma *et al.* 2021b), slope reinforcement (Jiang and Soga 2017), wind prevention and sand fixation (Duo *et al.* 2018, Zomorodian *et al.* 2019, Meng *et al.* 2021, Dagliya *et al.* 2022a, b, c), Heavy metal immobilization (Mwandira *et al.* 2017, Sharma *et al.* 2020, 2022).

In recent years, many scholars have carried out related researches on the mechanical properties of soil improved by MICP technology. Xiao *et al.* (2020) conducted one-dimensional compression test on calcareous sand treated with MICP to study the effects of particle gradation and $CaCO_3$ content on the compressive properties of calcareous sand. Khan *et al.* (2015) conducted tests on calcareous sand using the MICP technique and showed that the stiffness and strength of MICP treated calcareous sand samples were significantly improved compared to unprocessed calcareous sand samples. Zhao *et al.* (2021) studied the effect of fiber on the mechanical properties of calcareous sand treated by MICP through water absorption and unconfined compressive strength tests. Liu *et al.* (2018) used Ca^{2+} extracted from calcareous sand as a substitute for $CaCl_2$ to improve the mechanical properties of calcareous sand in the in MICP process. The above researches show that MICP technology has a good application in improving the mechanical properties of coarse-grained soils. Currently, with the improvement of MICP treatment process, the technique is also employed by some scholars to treat clay in order to improve the mechanical properties of clay. Kannan *et al.* (2020) provided insight into the effectiveness of the MICP technique in marine clay improvement through a series of index property tests. Teng *et al.* (2021) studied the effect of MICP process on clay using two different liquid addition methods, and evaluated the strength improvement of soil by unconfined compression test and micro cone penetration test. Cardoso *et al.* (2018) studied the effect of infiltration consolidation of clays on the permeability and tensile strength of soils and investigated the effect of clay chemical interactions on MICP. Liu *et al.* (2021) treated 5 groups of clayey soils with different sand content with MICP by surface spraying. In addition, the MICP technique has been used by some authors to improve the properties of loess (Atashgahi *et al.* 2020). The bacterial solution and cementation solution are poured into molds containing loose samples respectively in these research applications. And after multiple grouting, the samples strengthened by MICP showed higher strength with approximately four times the UCS of the untreated samples (Liu *et al.* 2021).

Studies on clay and loess have demonstrated that the MICP technique can also be applied in fine-grained soils with low permeability. However, few studies have been reported on the use of MICP technology to improve the Yellow River silt with small particle size and high sediment content. In the current situation of filling material shortage, it is meaningful to adopt MICP technology to treat the abandoned Yellow River silt into filling material. In addition, the process of soil solidification by MICP technology is affected by many factors, such as treatment time, pH and cementation solution concentration, etc. Therefore, further in-depth research is needed to investigate the mechanical properties in the Yellow River silt solidified by MICP technology.

MICP technology is employed to treat the Yellow River silt into filling material by means of peristaltic pump drip irrigation in this paper. A series of laboratory tests were carried out to study the effects of cementation solution concentration, treatment times and relative density on the solidification effect. The results of this paper are expected to provide technical support for improving the mechanical properties of Yellow River silt and realizing the resource utilization of silt.

2. Experimental materials and procedures

2.1 Experimental materials

2.1.1 Yellow River silt

The Yellow River silt used in this study were taken from the Yellow River beach near Zhengzhou, Henan Province, China, with a buried depth of about 4-8 m (Wang *et al.* 2022b). The soil particles in this area are loose, with high compressibility, poor adhesion between particles, and low strength, and the optimal water content is difficult to control. After the samples were taken back to the laboratory, they were dried in an oven at 105°C and vibrated evenly, and then their physical parameters were tested. Fig. 1 illustrates the particle size distribution of the Yellow River silt. The mass of particles with particle size greater than 0.075 mm accounts for 91.6% of the total mass according to the experimental results, which indicates that the silt is silty sand based on the standard (GBJ145-90). The basic physical parameters of the silt are listed in Table 1.

2.1.2 Bacteria

The bacterium selected for this paper was Sporosarcina pasteurii (DSM 33), purchased from the Institute of Microbiology, Chinese Academy of Sciences. It is screened from inside the natural soil, which is not harmful to the environment and has high urease activity, and is now widely adopted in the field of geotechnical engineering (Whiffin 2004, Van Panssen 2009, Liu *et al.* 2018, Xiao *et al.* 2021, Sharma *et al.* 2022a).

(1) Inoculation and culture of bacteria. A 500 mL liquid medium (10 g/L NH_4Cl, 20 g/L yeast extract powder, 24 mg/L $NiCl_2$•$6H_2O$, 12 mg/L manganese sulfate

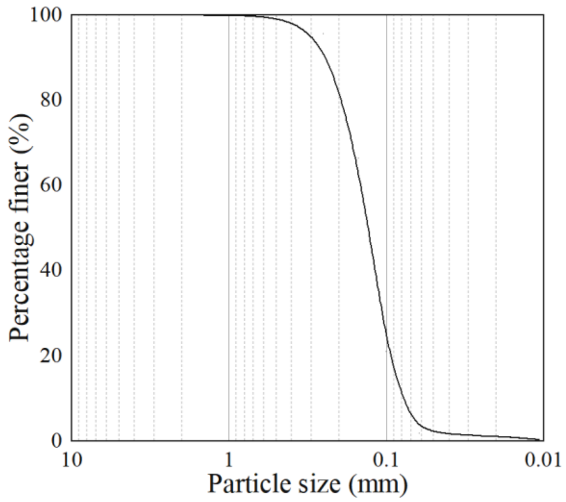

Fig. 1 Initial grain size distribution curve of silt

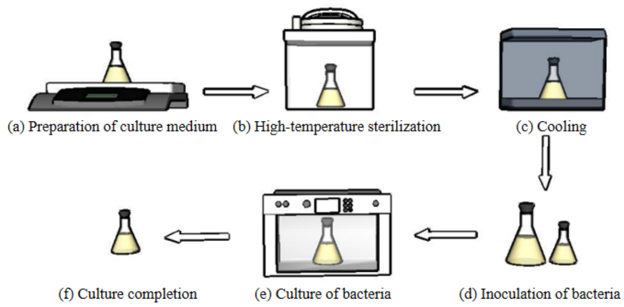

Fig. 2 Process of culturing bacteria

monohydrate) was prepared and the pH was adjusted to 9 with 1 mol/L NaOH (Meng *et al*. 2021). After the medium was configured, it was placed in an autoclave and autoclaved at 120°C for 60 min. When the medium was cooled to room temperature on a sterile operating table, the bacteria were inoculated into the medium at a ratio of 1:100 and incubated aerobically at 30°C using a constant temperature oscillating incubator at 150r/min. When the microorganisms are cultured to an optical density of 1.1 ~ 1.2, the bacteria can be harvested. The process of culturing bacteria is shown in Fig. 2.

(2) Measurement of urease activity. Under the action of urease, urea is hydrolyzed to produce carbonate and ammonium ions, so this process leads to the increase of solution conductivity. The amount of change in solution conductivity is proportional to the amount of urea hydrolysis. Therefore, the amount of urea hydrolysis per unit time can be used as an indicator of urease activity. The test method was as follows: 27 mL of urea solution (1.1 mol/L) was pipetted using a pipette gun and mixed well with 3 ml of the microbial solution to be tested, and the initial concentration of urea was 1 mol/L after mixing. At room temperature of 25°C, the conductivity meter (Remag DDB-303A type) was used to measure the conductivity of the solution every 5 minutes, and the change in conductivity of the solution was recorded for 15 min to calculate the average change in conductivity per minute. According to the correlation between the increase rate of conductivity and

Fig. 3 The real image after sample preparation

urea hydrolysis rate (Whiffin 2004), the amount of urea hydrolyzed by urease per minute (mM/min), i.e., the quantitative index of activity, was obtained. The activity of bacterial solution used in this test is 6.6 mM/min.

2.1.3 Cementation solution

The cementation solution used in this experiment were a mixture of $CaCl_2$ and urea, where urea provides nutrients for microbial growth and $CaCl_2$ is the source of calcium for the MICP process. Based on the basic equation of the reaction between urease hydrolysis and $CaCO_3$ deposition, the ratio of $CaCl_2$ to urea in the cementation solution is generally 1:1. In this experiment, eight different concentrations of cementation solution (0.25, 0.5, 0.75, 1.0, 1.25, 1.5, 1.75, 2.0 mol/L) were set up respectively to explore the influence of cementation solution concentration on the test (Deng *et al*. 2020).

2.2 Sample preparation

The Yellow River silt used in the test is dried in a drying oven and selected through a 2 mm sieve. The mold used for the test is a cylindrical mold, which is sealed by transparent tape. Besides, the bottom of the mold was perforated and padded with gauze in the lower part to prevent the leakage of silt particles. For sample preparation, the corresponding masses of silt were loaded into the molds and compacted in layers according to the set relative density (Dr=20%, 30%, 40%). The real image after sample preparation is provided in Fig. 3.

2.3 Test procedure and method

2.3.1 MICP treatment

In this test, the peristaltic pump drip irrigation solidification molding method is selected in the solidification molding process, and the device is shown in Fig. 4. After the samples were prepared, the fixative (0.05 mol/L$CaCl_2$) was instilled firstly into the samples by peristaltic pump and allowed to stand for 12h. The function of the fixative is to increase the fixation rate of microorganisms between particles by electrostatic adsorption of microorganisms (Harkes *et al*. 2009). After that, the samples are dripped with the cultured bacterial solution and left for 12h to allow the microorganisms to fully infiltrate and multiply in the silt. Subsequently,

Table 2 Experimental scheme of sediment silt

Sample number	Volume of bacterial solution (mL)	Volume of cementation solution (mL)	Relative density (%)	Cementation solution concentration (mol/L)	Treatment times
T-1~T-5	100	100	40%	0.25	2、4、6、8、10
T-6~T-10	100	100	40%	0.50	2、4、6、8、10
T-11~T-15	100	100	40%	0.75	2、4、6、8、10
T-16~T-20	100	100	40%	1.0	2、4、6、8、10
T-21~T-25	100	100	40%	1.25	2、4、6、8、10
T-26~T-30	100	100	40%	1.5	2、4、6、8、10
T-31~T-35	100	100	40%	1.75	2、4、6、8、10
T-36~T-40	100	100	40%	2.0	2、4、6、8、10
T-41~T-45	98	98	30%	1.0	2、4、6、8、10
T-46-T-50	96	96	20%	1.0	2、4、6、8、10
Control group A	0	100	40%	1.0	10
Control group B	100	0	40%	1.0	10

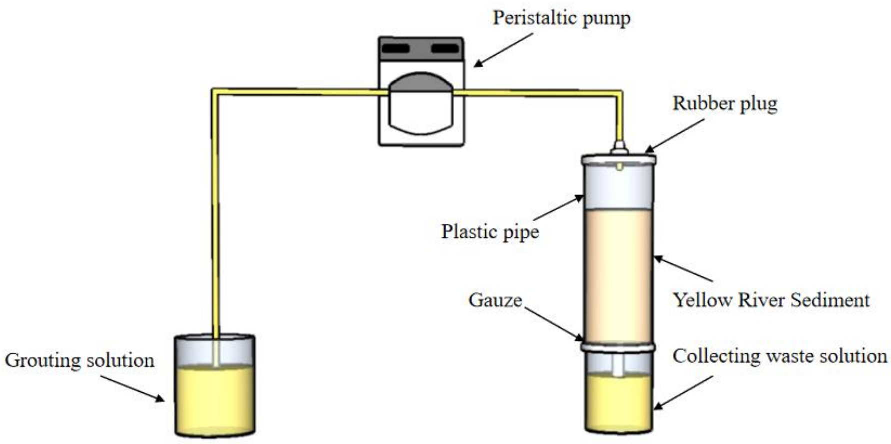

Fig. 4 Scheme of the Yellow River silt grouting test

the sample was filled with 1.2 times the volume of pore volume of cementation solution and left for 12 h to ensure the full reaction between the cementation solution and bacterial solution. The above operation was a single grouting, which was repeated several times in parallel. The detailed experimental scheme is shown in Table 2. In order to exclude irrelevant factors as well as to further demonstrate the role of bacteria in MICP, control group tests A and B were set up. In order to reduce the test error, three parallel specimens were set up for all test groups, with a total of 156 samples.

2.3.2 Unconfined compressive strength test

UCS test is to gradually apply axial pressure to the sample without any constraints until the sample is damaged. At this time, the pressure is UCS. Firstly, the samples treated by MICP are taken out of the mold and dried to a constant weight. Before testing, any unevenness are removed to ensure that it would be uniformly loaded. In order to reduce the test error, three samples are tested under each working condition. The instrument adopted in this test is the YYW-2 strain controlled unconfined pressure instrument purchased by Hohai University. The UCS of the samples were tested with a loading rate of 1.0 mm/min according to the Geotechnical Test Method Standard (GB/T 50123-1999).

2.3.3 Measurement of $CaCO_3$

After UCS test, the content of $CaCO_3$ was measured with the acid washing method. In order to explore the distribution of $CaCO_3$ in the sample, samples used in acid washing method were taken from the top, middle and bottom positions of the sample. The measurement steps are as follows:

(1) The test sample is selected from the upper part of the MICP-treated sample, and two samples are taken for each sample. The mass of the samples taken is controlled at 3 g in order to reduce the test error.

(2) The samples are dried to constant weight and weighed by electronic balance, m_1 and m_2, respectively.

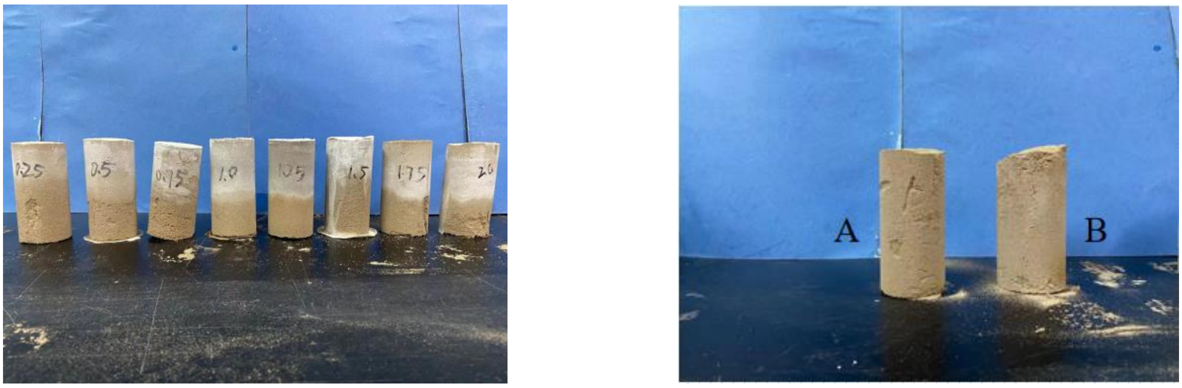

(a) Experimental group (b) Control group

Fig. 5 Sample diagram after MICP treatment

(3) The two samples are dissolved in 1 mol/L dilute hydrochloric acid solution and deionized water respectively. After standing for about ten minutes, the final volume of the solution shall be controlled at 50 ml.

(4) When there is no obvious bubbles in dilute hydrochloric acid solution, then stand for 1 h to ensure that $CaCO_3$ is completely dissolved.

(5) EDTA experiments are carried out on the solution of deionized water and dilute hydrochloric acid solution to obtain the calcium ion concentration.

(6) The percentage mass of $CaCO_3$ in the sample is obtained according to the following equation.

(7) According to the $CaCO_3$ content at different positions, the average calcium carbonate content of the whole sample can be calculated.

$$\omega = \left(\frac{c_1 V_1 M}{m_1} - \frac{C_2 V_2 M}{m_2} \right) \times 100\% \tag{3}$$

Where, ω is the percent mass content of $CaCO_3$ of the sample; c_1 and c_2 is the concentration of calcium ions in the solution after the sample is dissolved in dilute hydrochloric acid and deionized water respectively; V_1 is the volume of dilute hydrochloric acid solution; V_2 is the volume of deionized water; m_1 is the mass of the sample dissolved in dilute hydrochloric acid; m_2 is the mass of the specimen dissolved in deionized water.

2.3.4 Scanning electron microscope (SEM) test

The broken sample of UCS test is used for this experiment. The instrument model used in this experiment is Sigma 300. The diameter of the sample to be tested is controlled at about 50 mm and the height is less than 25 mm. It is very necessary to ensure the flatness of the lower bottom surface of each sample to be tested, so that the sample to be tested can be firmly bonded to the conductive paper. Before the experiment, the samples are dried in a 60°C oven and the surface is cleaned. In order to strengthen the conductivity of the sampels, vacuum gold spraying treatment is required before scanning. Finally, the micro morphologies of the sampels at different multiples such as 500, 1000 and 3000 are obtained by SEM, and photos were taken.

3. Results and analysis

3.1 Solidification molding of samples

It can be seen from Fig. 5(a) that the loose particles have basically bonded and formed, and the sample surface is smooth after the silt samples are treated by MICP. In the process of MICP, microorganisms mainly adhere to the particle surface due to the double electric layer structure of cell membrane and microbial secretion. The surface of microbial cell wall contains a large number of negative functional groups, and then adsorbs Ca^{2+} in the environment as the electron binding point. While the microorganism secretes urease to hydrolyze urea and continues to create an alkaline environment, the microorganism takes itself as the center to induce calcium carbonate precipitation. With the continuous formation of $CaCO_3$ and the continuous enhancement of the adhesion between particles, the loose particles finally form a whole with certain mechanical properties.

When only the cementation solution or bacteria is added to the mold, the surface of the sample is rough, and the upper part of control group B is obviously damaged during formwork removal. Since the samples of the control group have been damaged after formwork removal, the following contents will not conduct relevant tests on the samples of the control group. The results show that MICP solidified soil is the result of the joint action of bacteria and cementation solution.

3.2 Unconfined compressive strength

3.2.1 Effect of cementation solution concentration on UCS

Fig. 6 presents the UCS of the samples after ten times of treatment with different concentrations of cementation solution. Obviously, the cementation effect of MICP on samples increases first and then decreases with the increase of cementation concentration, which is consistent with the previous results reported by (Atashgahi *et al*. 2020). One possible reason is that urease activity is inhibited in the environment of high concentration of cementation solution. The UCS of the samples only increase from 25 kPa to 213 kPa, and the treatment effect is not ideal when the

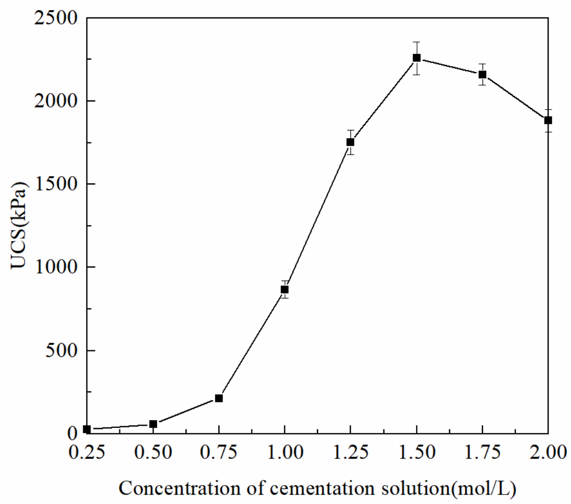

Fig. 6 Effect of cementation solution concentration on UCS of samples

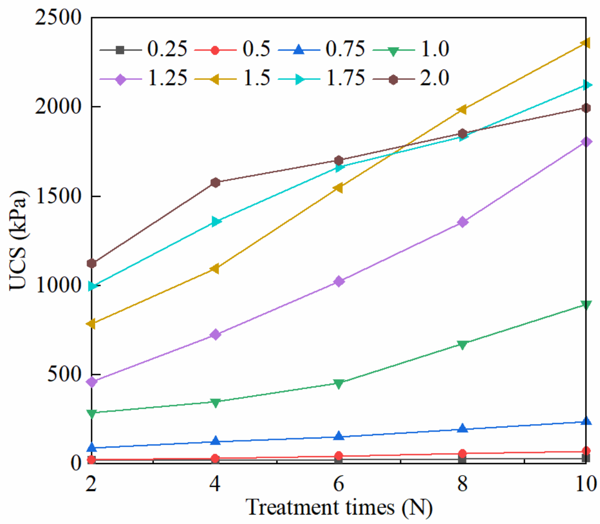

Fig. 7 Effect of treatment times on UCS of samples

concentration increases from 0.25 mol/L to 0.75 mol/L. Besides, UCS of samples increases slowly with the increase of the concentration of cementation solution. A main reason is that the $CaCO_3$ content induced by microorganisms is less and the size of $CaCO_3$ is small when the concentration is low. Due to the microorganisms generally adhere to the surface of small particles, most of the generated $CaCO_3$ exists around clay particles, and there is less $CaCO_3$ between clay aggregates and silt. Therefore, the cementation effect between them is poor, and the UCS of the samples is low. The UCS of the samples increases significantly when the concentration of cementation solution increases to 1mol/L, reaching 867 kPa. The UCS shows a continuous upward trend with the increase of the concentration of cementation solution to 1.5 mol/L and the maximum UCS reaches 2258 kPa. However, the UCS of the sample does not increase when the cementation solution concentration is greater than 1.5 mol/L, but shows a downward trend. Furthermore, the higher the concentration of cementation solution, the faster the UCS of the sample decreases. The reason may be that the higher concentration of cementation solution inhibits urease activity, resulting in insufficient Ca^{2+} and CO_3^{2-} to combine into $CaCO_3$ to cement silt particles (Wang *et al*. 2022b). In addition, it is also a possible reason that $CaCO_3$ is limited to a certain depth due to too fast reaction speed. In short, the concentration of cementation solution has an important influence on the process of MICP treatment. The concentration of the cementation solution can be chosen in the range of 1 mol/L to 1.5 mol/L.

3.2.2 Effect of treatment times on UCS

Fig. 7 shows the change of UCS of samples with treatment times under different cementation solution concentrations. The UCS of the sample does not increase significantly with the increase of treatment times when the concentration of cementation solution is low (less than 1mol/L). This is mainly because urease will quickly combine with substrate molecules after mixing with cementation solution. As a result, the cementation solution of each drip irrigation is consumed a lot in the upper part of

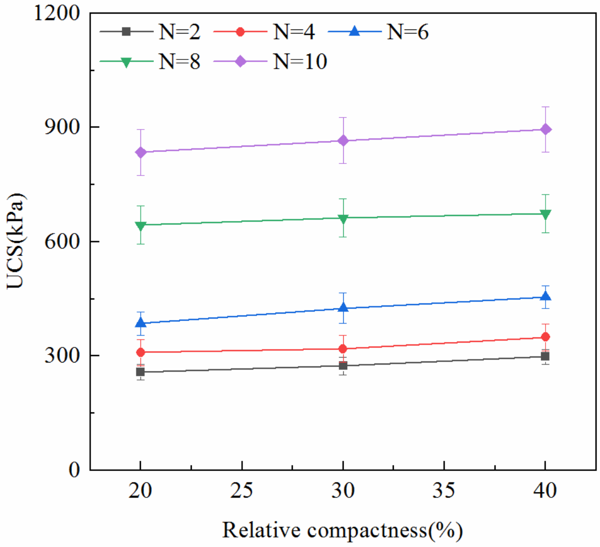

Fig. 8 Effect of relative density on UCS of samples

the sample, which is difficult to form effective cementation and is not enough to improve the UCS of the samples. When the concentration of cementation solution is increased to 1.0 mol/L~1.5 mol/L, the UCS of the sample increases significantly with the increase of treatment times, and the UCS of the sample with higher concentration of cementation solution increases faster. Moreover, the UCS of the samples still increases rapidly before being treated for 6 times when the concentration of cementation solution increases to 1.75 mol/L, but the upward trend of UCS slows down with the continuous increase of treatment times. This is because the bacteria have been saturated when the cementation solution concentration exceeds 1.75 mol/L, and the bacterial activity decreases slightly with the increase of the cement concentration. Besides, more $CaCO_3$ precipitation is generated between particles with the increase of treatment times. With the continuous growth of $CaCO_3$ crystal, microorganisms are gradually wrapped by $CaCO_3$ crystal. The restriction of nutrient transmission will lead to the decline of bacterial activity and even the death of bacteria, which is also one of the reasons for the slowdown of the upward trend of strength.

3.2.3 Effect of relative compactness on UCS

Fig. 8 demonstrates the effect of relative density of samples treated with 1 mol/L cementation solution on the UCS. It can be seen that the influence of relative density on UCS of MICP treated samples gradually increases with the increase of treatment times. After the samples are treated twice, the UCS of the samples with relative density of 20%, 30% and 40% are 259 kPa, 279 kPa and 286 kPa respectively. The UCS of medium dense silt (Dr = 40%) is about 9% higher than that of loose dense silt (Dr = 20%). After 10 treatments, the effect of relative density on the UCS of the sample is further enhanced. At this time, the UCS of medium dense silt (Dr = 40%) is about 15% higher than that of loose dense silt (Dr = 20%). When the treatment times are less, the amount of $CaCO_3$ produced is less, which is difficult to form effective cementation and is not enough to improve the UCS of samples. With the increase of treatment times, more $CaCO_3$ is produced, which can better bond the silt particles together, so that the UCS of the samples will be rapidly improved.

Besides, the greater the relative density, the higher the UCS of the samples. With the improvement of MICP treatment degree, the influence of relative density on the UCS of silt increases gradually. This is because the relative density also reflects the change of the sample porosity. With the increase of the relative density, the sample porosity decreases, and the dry density increases. The silt particles in the sample contact more closely. After MICP treatment, the contact between calcium carbonate and silt particles is more sufficient, so as to better cement the silt particles and improve the strength of the sample. The same conclusion was also proved by (lv,. 2021). It is worth mentioning that the influence of relative density on UCS is different for different sands. Compared with other results, the effect of relative density on the UCS is not particularly obvious due to the characteristics of the Yellow River silt used in this paper, such as many fine particles. After ten treatments, the UCS of the sample with a relative density of 40% is only about 50 kPa higher than that of the sample with a relative density of 20%. After ten treatments, the UCS of the sample with a relative density of 40% is only about 90 kPa higher than that of the sample with a relative density of 20%. In the case of the same gradation and $CaCO_3$, the UCS of the quartz sand sample with a relative density of 50% after MICP treatment can even be 0.5 MPa higher than that of the sample with a relative density of 30%. (Lv., 2021).

3.3 $CaCO_3$ content

3.3.1 Effect of cementation solution concentration on $CaCO_3$ content

Fig. 9 presents the effect of different cementation solution concentrations on the $CaCO_3$ content. In general, the test results of $CaCO_3$ content show that the $CaCO_3$ content of samples treated with different cementation solution concentration is different. The $CaCO_3$ content of

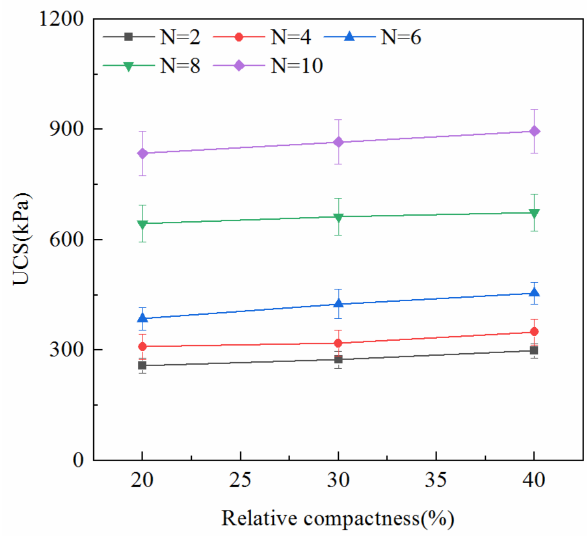

Fig. 8 Effect of relative compactness on UCS of samples

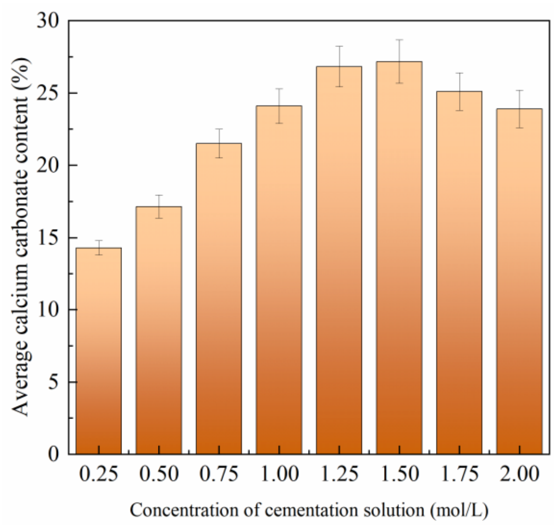

Fig. 9 Effect of cementation solution concentration on $CaCO_3$ content

the samples shows a gradual increase when the concentration of the cementation solution is from 0.25 mol/L to 1.5 mol/L. The samples treated with 1.5 mol/L of the cementation solution had the highest $CaCO_3$ content, up to 43% in the upper part. However, the $CaCO_3$ content in the samples gradually decreased when the concentration of the cementation solution is greater than 1.5 mol/L. This may be due to the inhibition of urease activity by the higher concentration of cementation solution, resulting in insufficient carbonate ions to combine with calcium ions and form $CaCO_3$. The change trend of $CaCO_3$ content of the sample is consistent with that of UCS combined with the above UCS test results. The UCS of the samples with high $CaCO_3$ content are also large, because the $CaCO_3$ crystal plays the role of cementation and filling between silt particles, which has a direct impact on the improvement of mechanical properties by MICP technology.

In addition, the results of UCS and $CaCO_3$ content of the sample show that when MICP technology is employed to solidify the silt, the treatment effect with appropriate high concentration within the cementation concentration range (1 mol/L~1.5 mol/L) is better. This means that the use of appropriate high concentration cementing fluid for microbial solidification of the Yellow River silt can achieve high mechanical properties. When reaching the mechanical indexes of the same goal, the use of relatively high concentration cementing fluid may greatly shorten the treatment time.

3.3.2 Effect of treatment times on $CaCO_3$ content

Fig. 10 illustrates the effect of treatment times on $CaCO_3$ content of samples. The test results show that the distribution and content of $CaCO_3$ are different in samples with different treatment times. The highest $CaCO_3$ content is found at the top of the sample because the treatment direction was top-down, and the $CaCO_3$ content decreased with increasing depth. After two treatments, the $CaCO_3$ content at the top and bottom of the sample was 10.1% and

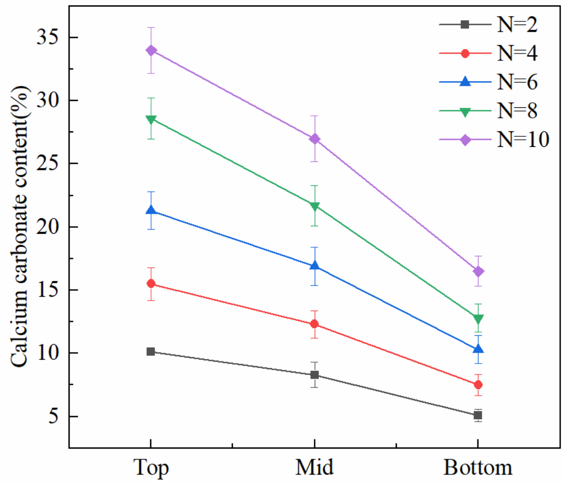

Fig. 10 Effect of treatment times on $CaCO_3$ content of samples

(a) T-6

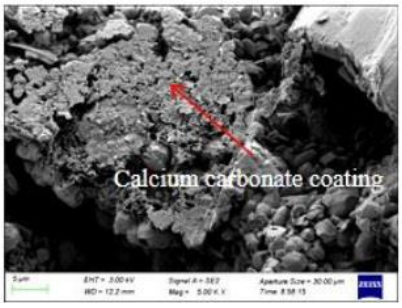

(b) T-10

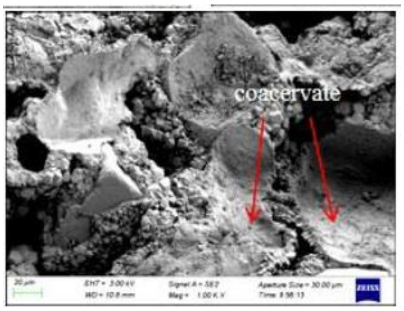

(c) T-16

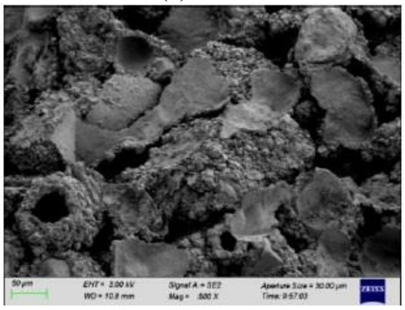

(d) T-20

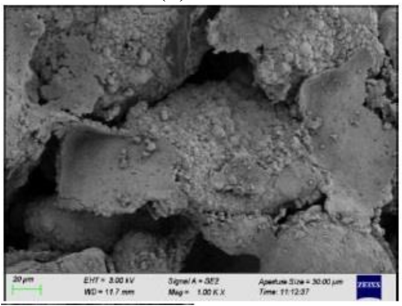

(e) T-45

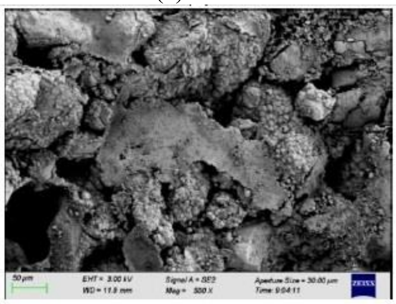

(f) T-50

Fig. 11 SEM image of samples after MICP treatment

5.1%, but after 10 treatments, the $CaCO_3$ content was for 34% and 16.5%, respectively. There are significant spatial differences in $CaCO_3$ content, which is mainly reflected in the decrease of $CaCO_3$ content with the increase of depth. Although the distribution of $CaCO_3$ is uneven, content of $CaCO_3$ in the whole sample increases with the increase of treatment times.

There are two main reasons for the less distribution of $CaCO_3$ in the lower part of the soil sample. On the one hand, the cementation solution infiltrates from the top to the bottom of the soil sample during the treatment process, but it will be preferentially adsorbed in the upper and middle parts of the soil sample, and relatively few urease migrate to the lower part. On the other hand, after a certain number of treatments, the content of $CaCO_3$ in the upper part of the samples is high, and most of the pores and particle surfaces of the soil sample are filled and cemented by $CaCO_3$. The seepage difficulty of the later treated cementation solution in the soil sample gradually increases, resulting in the reduction of urease penetrating to the lower part, so there is less $CaCO_3$ in the lower part.

3.4 Microstructure

The samples after MICP treatment were observed by SEM, and the results are shown in Fig. 11. Based on the results of SEM, the function and distribution of $CaCO_3$ crystals in the samples treated by MICP technology were discussed. According to the different depositional positions of $CaCO_3$, the role of $CaCO_3$ crystal can be divided into cementation and filling. Compared with the untreated Yellow River silt, the surface of the sample treated by MICP technique is covered with a large number of $CaCO_3$ crystals. Moreover, the stacking size of the generated

$CaCO_3$ crystals becomes larger with the progress of MICP calcification reaction. Some $CaCO_3$ crystals bond the silt particles with the silt particles, and the other $CaCO_3$ crystals fill the pores between the silt particles, so that the loose silt particles become a whole.

There are some differences in MICP treatment effects under different working conditions. Under the condition of constant treatment times and relative compactness, the cementation solution concentration has a significant effect during the MICP process. According to Fig. 11(a), the $CaCO_3$ crystal coating is thin when the concentration of cementation solution is 0.5 mol/L, and there is no large area of $CaCO_3$ crystals superimposed together. It can be seen from Fig. 11(c) that when the concentration of cementation solution is 1.0 mol/L, the coarse particles are completely wrapped by $CaCO_3$ crystals, and the fine particles are adsorbed on the surface of the coarse particles through their own cementation. Finally, the $CaCO_3$ coating is gradually superimposed into a bedding structure. As can be seen from Figs. 11(b) and 11(d), the rich $CaCO_3$ crystals produced after 10 treatments overlap and interweave on the surface of soil particles. The newly formed $CaCO_3$ crystals will adhere to the previously generated $CaCO_3$ precipitation with the increase of treatment times, the flaky clay particles will flocculate to form large soil aggregates, and the pores between the particles will be significantly reduced. It can be seen from Figs. 11(e) and 11(f) that the particles of the sample with relatively high compactness are more closely connected, and there is a large area of $CaCO_3$ crystal superposition, which explains the reason why the UCS of samples with high relative compactness is higher.

4. Conclusions

In this paper, MICP technology is employed to treat the Yellow River silt. The effects of cementation solution concentration, treatment times and relative density on the mechanical properties of the silt are studied. The UCS and $CaCO_3$ of the samples after MICP treatment were measured, and the microstructure of the samples was discussed. The following conclusions are made based on the research results:

- Microbial solution and calcium salt solution are the necessary conditions for MICP. After MICP treatment, the mechanical properties of the abandoned Yellow River silt are significantly improved, so that it can be used as high-quality filling material.
- The UCS of the Yellow River silt treated by MICP is significantly affected by the concentration of cementation solution and treatment times. The reasonable concentration of cementation solution is 1.5 mol/L. With the increase of treatment times, the pores in the soil are filled with $CaCO_3$, and the UCS of the specimens after 10 times of treatment can reach 2.5 MPa. Compared with the treatment times and concentration of cementation solution, the relative density has a weak effect on the UCS of samples.
- Under the treatment conditions of different cementation solution concentrations, the change trend of average $CaCO_3$ content in the sample is consistent with that of UCS. With the increase of treatment times, the content of $CaCO_3$ induced by microorganisms increased continuously. When the concentration of the cementation solution is 1.5 mol/L, the $CaCO_3$ content of the sample treated by MICP technology is the highest.
- According to the SEM results, $CaCO_3$ crystals occur on the surface of the sample treated by MICP, and the pores in the samples are filled with $CaCO_3$ induced by microorganisms. The stacking size of $CaCO_3$ crystals becomes larger with the increase of cementation solution concentration and treatment times, so the connection between particles is closer and the strength of samples is continuously improved.

Acknowledgements

The work present in this paper was supported by National Natural Science Foundation of China (Grant No. 52178369; 52109140); Key Projects of High Schools of Henan province (20A560021); Natural Science Foundation of Henan Province (202300410424); Youth Talent Promotion Project of Henan Province (2021HYTP016); Key Specialized Research and Development Breakthrough in Henan Province (212102310977); China Postdoctoral Science Foundation (2019M662533). These financial supports are gratefully acknowledged.

References

Atashgahi, S., Tabarsa, A., Shahryari, A. and Hosseini, S. (2020), “Effect of carbonate precipitating bacteria on strength and hydraulic characteristics of loess soil”, *Bull. Eng. Geol. Environ.*, **79**(9), 4749-4763. https://doi.org/10.1007/s10064-020-01857-0.

Atefeh, Z., Xiao, P., Baumer, T., Carey, T.J., Sawyer, B., Dejong, J.T. and Boulanger, R.W. (2021), “Mitigation of liquefaction triggering and foundation settlement by MICP treatment”, *J. Geotech. Geoenviron. Eng.*, 147(10). https://doi.org/10.1061/(ASCE)GT.1943-5606.0002596.

Burbank, M., Weaver, T., Green, T., Williams, B. and Crawford, R. (2011), “Precipitation of calcite by indigenous microorganisms to strengthen liquefiable soils”, *Geomicrobio. J.*, **28**(4). https://doi.org/10.1080/01490451.2010.499929.

Cardoso, R., Pires, I., Duarte, S. and Monteiro, G. (2018), “Effects of clay's chemical interactions on biocementation”, *Appl. Clay Sci.*, **156**, 96-103. https://doi.org/10.1016/j.clay.2018.01.035.

Choi, S., Chu, J. and Kwon, T. (2019), “Effect of chemical concentrations on strengthand crystal size of biocemented sand”, *Geomech. Eng.*, **17**(5), 465-473. https://doi.org/10.12989/gae.2019.17.5.465.

Dagliya, M., Satyam, N. and Garg, A. (2022b), “Experimental Study on Optimization of Cementation Solution for Wind-Erosion Resistance Using the MICP Method”, Sustainability (Switzerland), 14. https://doi.org/10.3390/su14031770.

Dagliya, M., Satyam, N. and Garg, A. (2022c), “Biopolymer based stabilization of Indian desert soil against wind-induced erosion”, *Acta Geophysica*. https://doi.org/10.1007/s11600-022-00905-5.

Dagliya, M., Satyam, N., Sharma, M. and Garg, A. (2022a), “Experimental study on mitigating wind erosion of calcareous desert sand using spray method for microbially induced calcium carbonate precipitation”, *J. Rock Mech. Geotech. Eng.*, 1-12.

https://doi.org/10.1016/j.jrmge.2021.12.008.

DeJong, J., Mortensen, B., Martinez, B.C. and Nelson, D.C. (2008), "Bio-mediated soil improvement", *Ecological Eng*., **36**(2), 197-210. https://doi.org/10.1016/j.ecoleng.2008.12.029.

Deng, X., Yuan, Z., Li, Y.u., Liu, H., Feng, J. and de Wit, B. (2020), "Experimental study on the mechanical properties of microbial mixed backfill", *Constr. Build. Mater*., **265**, 120643. https://doi.org/10.1016/j.conbuildmat.2020.120643.

Hang, L., Gao, Y., He, J. and Chu, J. (2019), "Mechanical behaviour of biocemented sand under triaxial consolidated undrained or constant shear drained conditions", *Geomech. Eng*., **17**(5), 497-505. https://doi.org/10.12989/gae.2019.17.5.497.

Harkes, M.P., van Paassen, L.A., Booster, J.L., Whiffin, V.S. and van Loosdrecht, M.C.M. (2009), "Fixation and distribution of bacterial activity in sand to induce carbonate precipitation for ground reinforcement", *Ecological Eng*., **36**(2), 112-117. https://doi.org/10.1016/j.ecoleng.2009.01.004.

Jiang, N. and Soga, K. (2017), "The applicability of microbially induced calcite precipitation (MICP) for internal erosion control in gravel–sand mixtures", *Géotechnique*, **67**(1), 42-55. https://doi.org/10.1680/jgeot.15.P.182.

Kannan, K., Bindu, J. and Vinod, P. (2020), "Engineering behaviour of MICP treated marine clays", *Mar. Georesour. Geotech*., **38**(7), 1-9. https://doi.org/10.1080/1064119X.2020.1728791.

Khan, M., Amarakoon, G., Shimazaki, S. and Kawasaki, S. (2015), "Coral sand solidification test based on microbially induced carbonate precipitation using ureolytic bacteria", *Mater. Transactions*, **56**(10), 1725-1732. https://doi.org/10.2320/matertrans.M-M2015820.

Li, D., Tian, K., Zhang, K., Wu, Y. and Nie, K. (2018), "Experimental investigation of solidifying desert aeolian sand using microbially induced calcite precipitation", *Constr. Build. Mater*., **172**, 251-262. https://doi.org/10.1016/j.conbuildmat.2018.03.255.

Liu, B., Xie, Y.H., Tang, C.S., Pan, X.H., Jiang, N.J. and Singh, D. (2021), "Bio-mediated method for improving surface erosion resistance of clayey soils", *Eng. Geol*., **293**(19), 106295. https://doi.org/10.1016/j.enggeo.2021.106295.

Liu, L., Liu, H., Xiao, Y., Chu, J., Xiao, P. and Wang, Y. (2018), "Biocementation of calcareous sand using soluble calcium derived from calcareous sand", *Bull. Eng. Geol. Environ*., **77**(4), 1781-1791. https://doi.org/10.1007/s10064-017-1106-4.

Liu, X., Fan, J., Jing, Y.U. and Xin, G. (2021), "Solidification of loess using microbial induced carbonate precipitation", *J. Mountain Sci*., **18**(1), 265-274. https://doi.org/10.1007/s11629-020-6154-8.

Lv, Y. (2021), "Experimental study on mechanical and permeability properties of fiber-reinforced bio-cement sand with different gradation", Chongqing University. (in Chinese).

Mahawish, A., Bouazza, A. and Gates, W. (2019), "Unconfined compressive strength and visualization of the microstructure of coarse Sand subjected to different biocementation levels", *J. Geotech. Geoenviron. Eng*., **145**(8), 1943-1956. https://doi.org/10.1061/(ASCE)GT.1943-5606.0002066.

Meng, H., Gao, Y., He, J., Qi, Y. and Hang, L. (2021), "Microbially induced carbonate precipitation for wind erosion control of desert soil: Field-scale tests", *Geoderma*, 383. https://doi.org/10.1016/j.geoderma.2020.114723.

Montoya, B. and DeJong, J. (2015), "Stress-strain behavior of sands cemented by microbially induced calcite precipitation", *J. Geotech. Geoenviron. Eng*., **141**(6), 1943-1953. https://doi.org/10.1061/(ASCE)GT.1943-5606.0001302.

Montoya, B., Dejong, J. and Boulanger, R. (2013), "Dynamic response of liquefiable sand improved by microbial-induced calcite precipitation", *Géotechnique*, **63**(4), 302-312. https://doi.org/10.1680/geot.SIP13.P.019.

Mwandira, W., Nakashima, K. and Kawasaki, S. (2017), "Bioremediation of lead-contaminated mine waste by Pararhodobacter sp. based on the microbially induced calcium carbonate precipitation technique and its effects on strength of coarse and fine grained sand", *Ecological Eng*., **109**, 57-64. https://doi.org/10.1016/j.ecoleng.2017.09.0111.

Paassen, L.A., Ghose, R., van der Linden, T.J.M., van der Star, W.R.L. and van Loosdrecht, M.C.M. (2010), "Quantifying biomediated ground improvement by ureolysis: Large-scale biogrout experiment", *J. Geotech. Geoenviron. Eng*., **136**(12), 1721-1728. https://doi.org/10.1061/(ASCE)GT.1943-5606.0000382.

Sharma, M., Satyam, N. and Reddy, K.R. (2020), "Strength enhancement and lead immobilization of sand using consortia of bacteria and Blue-Green Algae", *J Hazardous, Toxic, and Radioactive Waste (ASCE)*, **24**, 04020049. https://doi.org/10.1061/(ASCE)HZ.2153-5515.0000548.

Sharma, M., Satyam, N. and Reddy, K.R. (2021b), "Effect of freeze-thaw cycles on engineering properties of biocemented sand under different treatment conditions", *Eng. Geol*., **284**, 106022. https://doi.org/10.1016/j.enggeo.2021.106022.

Sharma, M., Satyam, N. and Reddy, K.R. (2022a), "Large-scale spatial characterization and liquefaction resistance of sand by hybrid bacteria induced biocementation", *Eng. Geol*., **302**, 106635. https://doi.org/10.1016/j.enggeo.2022.106635.

Sharma, M., Satyam, N. and Reddy, K.R. (2022b), "Liquefaction resistance of biotreated sand before and after exposing to weathering conditions", *Indian Geotech. J*., **52**, 328-340. https://doi.org/10.1007/s40098-021-00576-x.

Sharma, M., Satyam, N., Reddy, K.R. and Chrysochoou, M. (2022c), "Multiple heavy metal immobilization and strength improvement of contaminated soil using bio-mediated calcite precipitation technique", *Environ. Sci. Pollut. Res*., https://doi.org/10.1007/s11356-022-19551-x.

Simatupang, M., Okamura, M., Hayashi, K. and Yasuhara, H. (2018), "Small-strain shear modulus and liquefaction resistance of sand with carbonate precipitation", *Soil Dyn. Earthq. Eng*., **115**, 710-718. https://doi.org/10.1016/j.soildyn.2018.09.027.

Teng, F., Sie, Y. and Ouedraogo, C. (2021), "Strength improvement in silty clay by microbial-induced calcite precipitation", *Bull. Eng. Geol. Environ*., **80**(8), 1-13. https://doi.org/10.1007/s10064-021-02308-0.

Wang, Y., Cao, T., Gao, Y. and Shao, J. (2022a), "Experimental study on liquefaction characteristics of saturated Yellow River silt under cycles loading", *Soil Dyn. Earthq. Eng*., **163**, 107457. https://doi.org/10.1016/j.soildyn.2022.107457.

Wang, Y., Wang, G., Wan, Y., Yu, X., Zhao, J. and Shao, J. (2022b), "Recycling of dredged river silt reinforced by an eco-friendly technology as microbial induced calcium carbonate precipitation (MICP)", *Soils Found*., **62**, 101216. https://doi.org/10.1016/j.sandf.2022.101216.

Whiffin, V.S. (2004), "Microbial $CaCO_3$ precipitation for the production of biocement", Perth West Australia: Morduch University.

Xiao, Y., Chen, H., Stuedlein, A., Evans, T., Chu, J., Cheng, L., Jiang, N., Lin, H., Liu, H. and Aboel-naga, H.M. (2020), "Restraint of particle breakage by biotreatment method", *J. Geotech. Geoenviron. Eng*., **146**(11). https://doi.org/10.1061/(ASCE)GT.1943-5606.0002384.

Zamani, A., Xiao, P., Baumer, T. and Caray, T. (2021), "Mitigation of Liquefaction Triggering and Foundation Settlement by MICP Treatment", *J. Geotech. Geoenviron. Eng*., **147**, 04021099. https://doi.org/10.1061/(asce)gt.1943-5606.0002596.

Zhao, J., Tong, W., Shan, Y., Yuan, J., Peng, Q. and Ling, J. (2021), "Effects of different types of fibers on the physical and mechanical properties of MICP-treated calcareous sand",

Materials, **14**(2). https://doi.org/10.3390/ma14020268.
Zomorodian, S.M.A., Ghaffari, H. and Kelly, B.C. (2019), "Stabilisation of crustal sand layer using biocementation technique for wind erosion control", *Aeolian Res.*, **40**, 34-41. https://doi.org/10.1016/j.aeolia.2019.06.001.

CC

Nomenclature

ω_L (%)	Liquid limit
ω_P (%)	Plastic limit
G_s	The particle density
ρ_{dmax} ($g \cdot cm^{-3}$)	Maximum dry density
$\rho_{\mathrm{d\,min}}$ ($g \cdot cm^{-3}$)	Minimum dry density
e_{max}	Maximum void ratio
e_{min}	Minimum void ratio